A compact wide band textile MIMO antenna with very low mutual coupling for wearable applications

Article *in* International Journal of RF and Microwave Computer-Aided Engineering · April 2019

DOI: 10.1002/mmce.21769

2 authors:

Ashim Kumar Biswas
National Institute of Technology, Silchar
11 PUBLICATIONS **3** CITATIONS
SEE PROFILE

Ujjal Chakraborty
National Institute of Technology, Silchar
36 PUBLICATIONS **226** CITATIONS
SEE PROFILE

Received: 24 January 2019 | Revised: 14 March 2019 | Accepted: 23 March 2019

DOI: 10.1002/mmce.21769

RESEARCH ARTICLE

INTERNATIONAL JOURNAL OF RF AND MICROWAVE COMPUTER-AIDED ENGINEERING WILEY

A compact wide band textile MIMO antenna with very low mutual coupling for wearable applications

Ashim Kumar Biswas | **Ujjal Chakraborty**

Department of Electronics and Communication Engineering, National Institute of Technology, Silchar, Assam, India

Correspondence
Ashim Kumar Biswas, Department of ECE, National Institute of Technology, Silchar, Assam, India.
Email: ashim10@gmail.com

Abstract

This communication presents a compact wide band wearable MIMO antenna with very low mutual coupling (VLMC). The proposed antenna is composed of Jeans material. Two "I" shaped stubs are connected in series and are employed on the ground plane between the two patches separated by 0.048 λ to increase isolation characteristics of the antenna-port. The antenna covers frequency spectrum from 1.83 GHz to 8 GHz (about 125.5%) where the minimum port isolation of about 22 dB at 2.4 GHz and maximum of about 53 dB at 5.92 GHz are obtained. The envelope correlation coefficient (ECC) of the MIMO antenna is obtained to be less than 0.01 with a higher diversity gain (DG > 9.6) throughout the whole operating band. The proposed MIMO antenna is cost effective and works over a wide frequency band of WLAN (2.4-2.484 GHz/5.15-5.35 GHz/5.72-5.825 GHz), WiMAX (3.2-3.85 GHz) and C-band downlink-uplink (3.7-4.2 GHz/5.925-6.425 GHz) applications. Simulation results are in well agreement with the measurement results.

KEYWORDS

envelope correlation coefficient (ECC), textile MIMO antenna, total active reflection coefficient (TARC), very low mutual coupling (VLMC), wearable antenna

1 | INTRODUCTION

Recently, there has been an enormous demand of high-performance compact antenna for wearable devices. The idea of these wearable antennas has widespread in the arenas of rescue in urgent crisis condition, monitoring of health, medical assistance, and physical training applications.[1] The demanding high data rate needs additional antenna elements that may increase the functional capability for the multiple frequency applications. On the other hand, recent wireless devices also require the system miniaturization along with the multi-antenna arrangements.[2] Therefore, researchers should take care for the design of the recent wireless gadgets. In this perspective, wide band MIMO antennas are found to be essential because of their less power requirement, ability to provide extraordinary data rate and exclusion from the interferences of other schemes.[3,4] The design of a wearable antenna is really challenging due to its operation in human-body that consists of a lossy intermediate with a high value of permittivity. The efficiency of the antenna may be degraded by this property.[5] Therefore, special precaution is to be set due to its textile integrated wearable design.[6–8] Different real-world circumstances such as folding, twisting, and washing disputes are also possible for the wearable on-body antenna performance.[9] Insertion of EBG, SRR, different stubs, slots, DGS into the MIMO antenna could advance the antenna performances such as gain improvement, broaden of bandwidth and mutual coupling (MC) reduction between the elements.[10,11] MIMO antenna can increase the transmission ability as well improve the spectral efficiency. It also simplifies the layers of the multiple accesses and upturns the robustness along with the reduction of the air interface potential.[12] Reduction of mutual coupling is one of the major constraints in MIMO antenna design.[13] It is also desired that the envelope correlation coefficient (ECC) should be very low along with higher diversity gain

(DG) for a good MIMO antenna system. Any wearable scheme that is durable and efficiently communicates is more suitable and trustworthy to use. This will be more helpful upon most suffering circumstances.[14] In these contexts, design of wearable MIMO antenna is very much important.

A number of wearable MIMO antennas with high port isolation have been reported in various literatures for the wireless applications.[5,15–18] A wearable MIMO antenna that operates in the frequency spectrum from 2.4 GHz to 2.49 GHz for wireless local area network application is presented in Reference 5. It is reported that the design could achieve about 15 dB of port isolation. In Reference 15, a wearable MIMO antenna for WLAN application is proposed. The antenna uses ground radiation with polarization diversity characteristics. The article has presented the port isolation of 20 dB with a very low bandwidth of 140 MHz. A single-layer compact textile MIMO antenna has been described in Reference 16, for wearable applications. The reported port isolation is about 12 dB. A textile dual band MIMO antenna based on the substrate integrated waveguide structure has been proposed in Reference 17, to achieve the port isolation of 18 dB in lower band and 35 dB in upper band. In Reference 18, a dual band MIMO antenna for wearable device supporting the 5G radio frequency from 3.3 GHz to 3.6 GHz and 4.5 GHz to 5 GHz has been presented. The extreme port isolation as conveyed in that paper is about 17 dB.

In this article, the reduction of mutual coupling of a dual-port MIMO antenna containing two simple rectangular fashioned antenna elements is investigated. The antenna consists of a partially etched ground plane. It is integrated with two 'I'-shaped stubs connected in series and located on the back surface. The proposed antenna provides the wide frequency spectrum from 1.83 GHz to 8 GHz covering a number of well-recognized frequency bands such as WLAN, WiMAX, and C-band downlink and uplink applications. We have obtained very low envelope correlation coefficient (ECC < 0.01), nominal value of channel capacity loss (CCL < 01.9 BPS/Hz) and higher diversity gain (DG > 9.6) from the exploration of the antenna. In this proposed prototype, good steady radiation patterns are observed throughout the complete operating band. The antenna is simulated, analyzed, and optimized with the help of Ansys High Frequency Structure Simulator (HFSS).[19] The simulated results are found to be well matched with that of the measured results using the fabricated prototype. The rest of the article is arranged as; the detail design method of the antenna is conversed in Section 2, simulated and measurement results are conversed in Section 3 followed by drawing a concise conclusion in Section 4.

2 | ANTENNA STRUCTURE AND DESIGN

The top view of the proposed antenna geometry is depicted in Figure 1A. The MIMO antenna is constructed by placing two rectangular copper patch elements on a low cost easily obtainable Jeans material. The material has the permittivity (ε_r) of 1.6 and loss tangent (tan δ) of 0.02. The height (h) of the stacked Jeans substrate is fixed at 1 mm. The dielectric property of the substrate is found using the procedure specified in Reference 20. These substrate parameters are optimized by the simulation of two simple rectangular patch antenna elements that are placed on the same Jeans substrate. The complete size of the antenna is 0.56 $\lambda \times 0.32\ \lambda \times 0.008\ \lambda$. The proposed MIMO structure is integrated with two etched 'I' shaped stubs interconnected in series and organized on the ground surface to improve the port isolation.

The ground layers of the MIMO antenna without stub and with stub are demonstrated in Figures 1B and 2B respectively. The topmost view of the antenna shows the feeding mechanism of the dual antenna elements along with their port positions and the back layer displays a modified ground structure. The separation among the two antenna elements is about 0.048 λ. The reduction of mutual coupling appeared between the two ports is obtained by implementing two "I" shaped stubs connected in series on the ground surface (as shown in Figure 2C). The dimension of the proposed MIMO antenna parameters are summarized in Table 1.

2.1 | MIMO antenna with single 'I' shaped stub

To attain the final design, we have examined some parametric variations. At the beginning, a simple MIMO antenna is designed which consists of two rectangular patch elements on the top surface of the substrate Jeans material. The antenna is simulated by Ansys HFSS and examined experimentally. It reveals frequency band from 1.85 to 5.87 GHz. However, it shows a poor port isolation of which needs to be improved. In this process, an 'I' shaped stub is placed on the ground plane as exposed in Figure 2A. The design is further scrutinized to improve the mutual coupling, which is discussed in the following sections.

2.2 | MIMO antenna with double 'I' shaped stub connected in series

In the second iteration, one more 'I' shaped stub is connected in series with the previous stub as shown in Figure 2B. This new one is investigated to produce very low mutual coupling (VLMC) between the ports. Optimized parameter values of the two "I" shaped stubs are indicated in Figure 2C and Table 1. This proposed antenna offers the wide frequency spectra from 1.83 to 8 GHz with very high port isolation as shown in Figure 3. In comparison of reflection coefficient parameters for a single and double 'I' shaped stubs, we observed that the slight enhancement in the antenna bandwidth is due to the

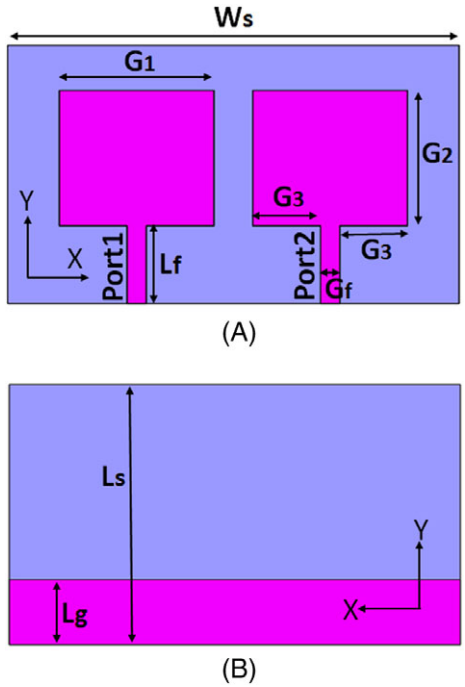

FIGURE 1 Arrangement of the MIMO antenna (A) top view and (B) bottom view

change in the quality factor of antenna. The strategy to introduce the "I" shaped stub on the antenna structure is based on the microstrip filtering mechanism. The stub along with the gap creates a capacitive and inductive environment to form an equivalent stop band filtering inside the structure. Thus the suitable insertion of the 'I' shaped stubs on the ground plane reduces the current flowing from the excitation port towards the coupled port. This helps to cancel the electromagnetic coupling of the second radiator and ensures very high port isolation.

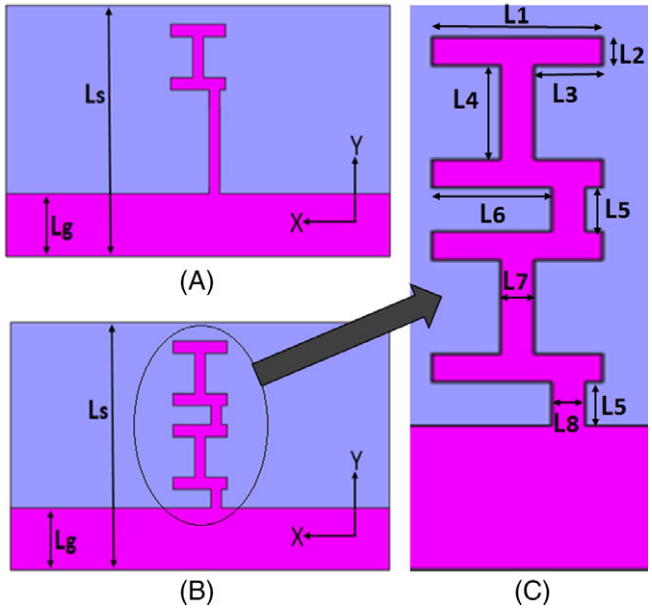

FIGURE 2 Bottom layer of MIMO antenna with (A) single 'I' stubs, (B) double 'I' stub, and (C) structure of the double 'I' stub

TABLE 1 Parameter dimension of the proposed MIMO antenna

Parameters	Dimension (mm)	Parameters	Dimension (mm)
G_1	24	L1	10
G_2	21	L2	2
G_3	10.5	L3	4
G_f	3	L4	6.5
L_f	12	L5	3
Ws	70	L6	7
Lg	10	L7	2
Ls	40	L8	2
d	6	h	1

3 | RESULTS WITH EXPLANATIONS

The double element textile MIMO antenna (with and without stub) structures are fabricated manually using a section of copper foil with 0.07 mm thickness. The front and back view are depicted in Figure 4A-D. Two 50Ω subminiature A (SMA) connectors are used for the excitation to the antenna elements. The simulated results and performances along with the measured outcomes are discussed in the proceeding subsections.

3.1 | Scattering parameters

The measured and simulated scattering parameters of the prototype without stub are illustrated in Figure 5. The simulated one covers the frequency spectrum from 1.49 to

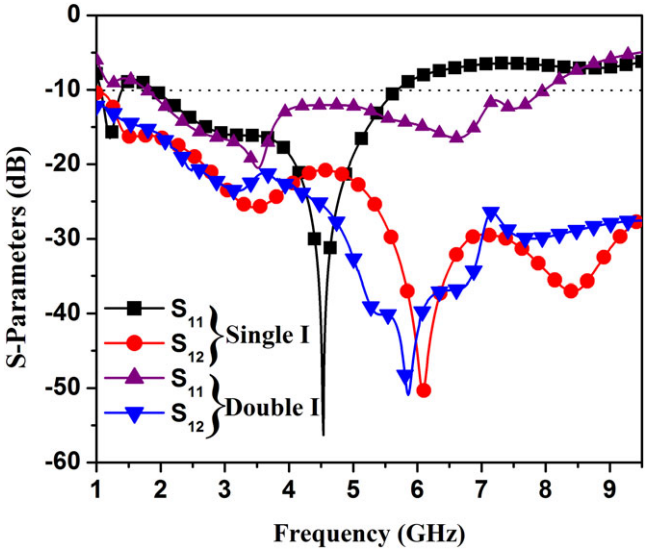

FIGURE 3 The scattering parameters of the MIMO antenna with single 'I' and double 'I' shaped stub on the ground plane

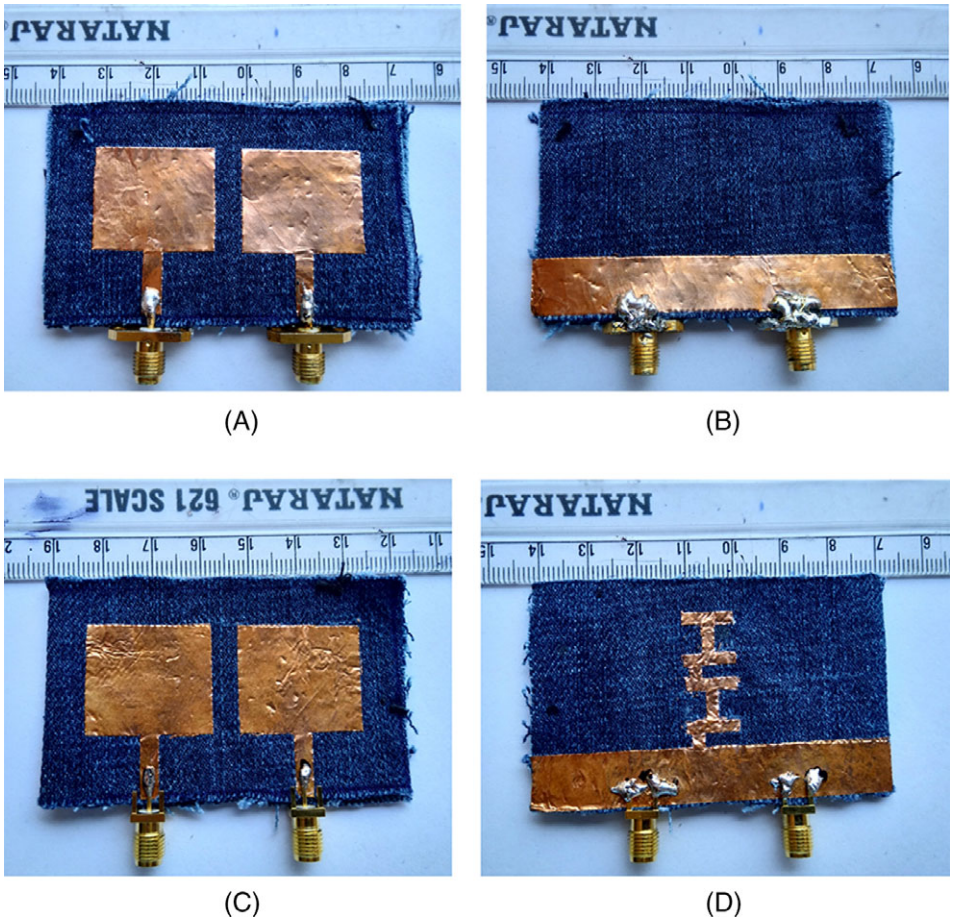

FIGURE 4 Fabricated MIMO antenna (A) top view, (B) bottom view without stub, and (C) top view, (D) bottom view with stub

5.87 GHz whereas the measured bandwidth is obtained from 1.23 to 6.51 GHz (for $S_{11} \leq -10$ dB). Again, we compare the S-parameters (S_{11} and S_{12}) when two stubs are used on the backside of the proposed MIMO antenna. The measured and simulated frequency ranges are 1.2 to 8 GHz and 1.83 to 8 GHz respectively (for $S_{11} \leq -10$ dB). The simulated results are found to be almost matched with the measured results as illustrated in Figures 5 and 6.

The insertion of the double 'I' shaped stubs on the ground layer of the MIMO antenna has increased the −10 dB

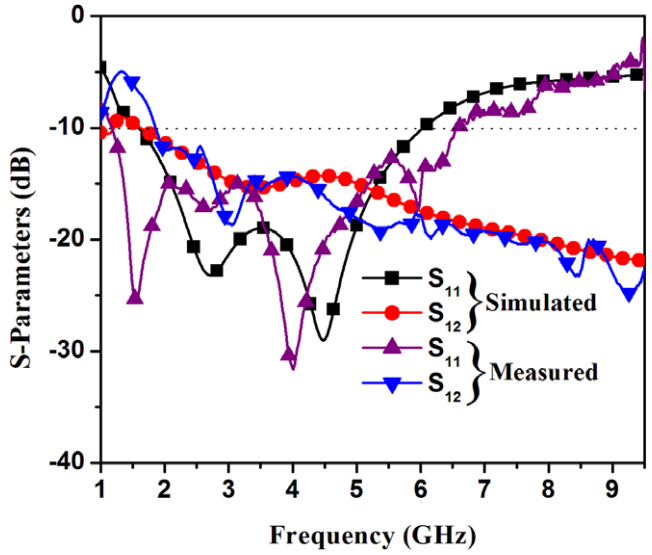

FIGURE 5 Simulated and measured S-parameters of the MIMO antenna with the absence of stub on ground plane

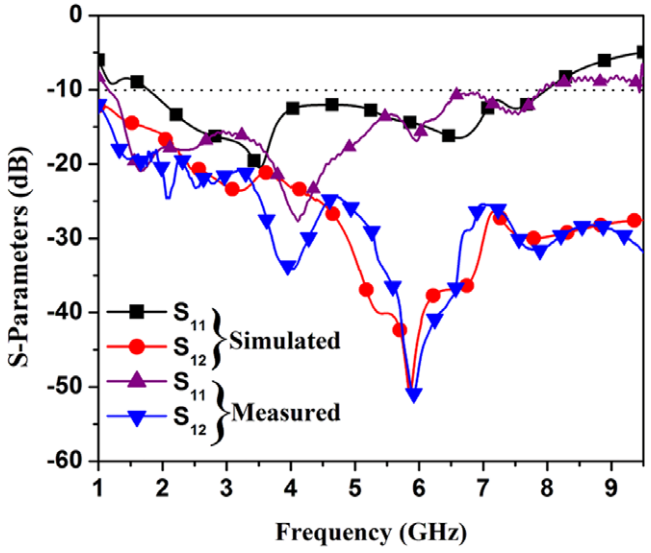

FIGURE 6 Simulated and measured S-parameters of the proposed antenna with double stub on ground plane

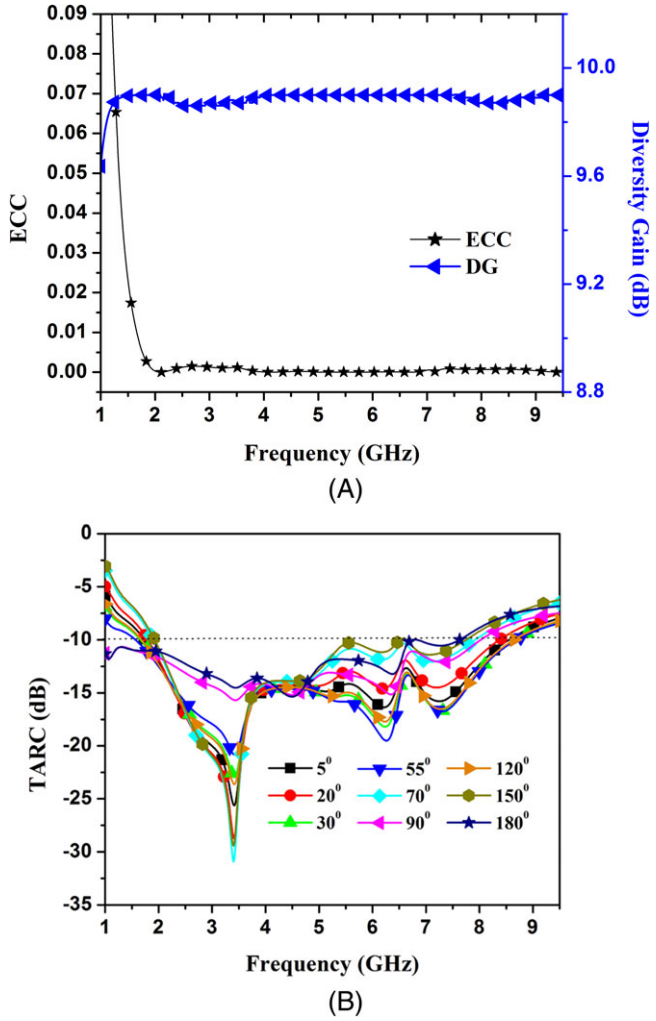

FIGURE 7 (A) The variation of ECC and diversity gain of the antenna with frequency (B) TARC curve of the proposed MIMO antenna

bandwidth and moved up the resonant frequency by 2.13 GHz (Figure 3). The change in the effective inductance and capacitance are occurred by modifying the distance between the exposed end of the stub and the ground plane. It results in reduction of the antenna quality factor, which in turn enhances the bandwidth of the antenna. This stub improves the measured port isolation up to 13 dB at 2.4 GHz and 36.5 dB at 5.92 GHz, which also approve the acceptability of the simulation results. The minor inconsistency may be due to the manufacturing tolerances like slightly parametric variations.

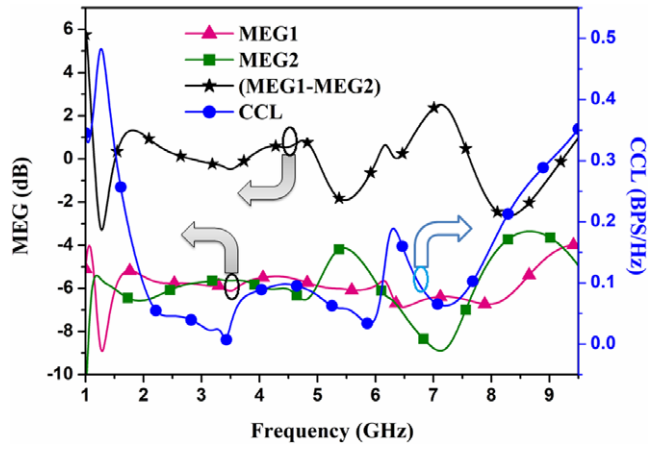

FIGURE 8 The variation of channel capacity loss and mean effective gain of the antenna with frequency

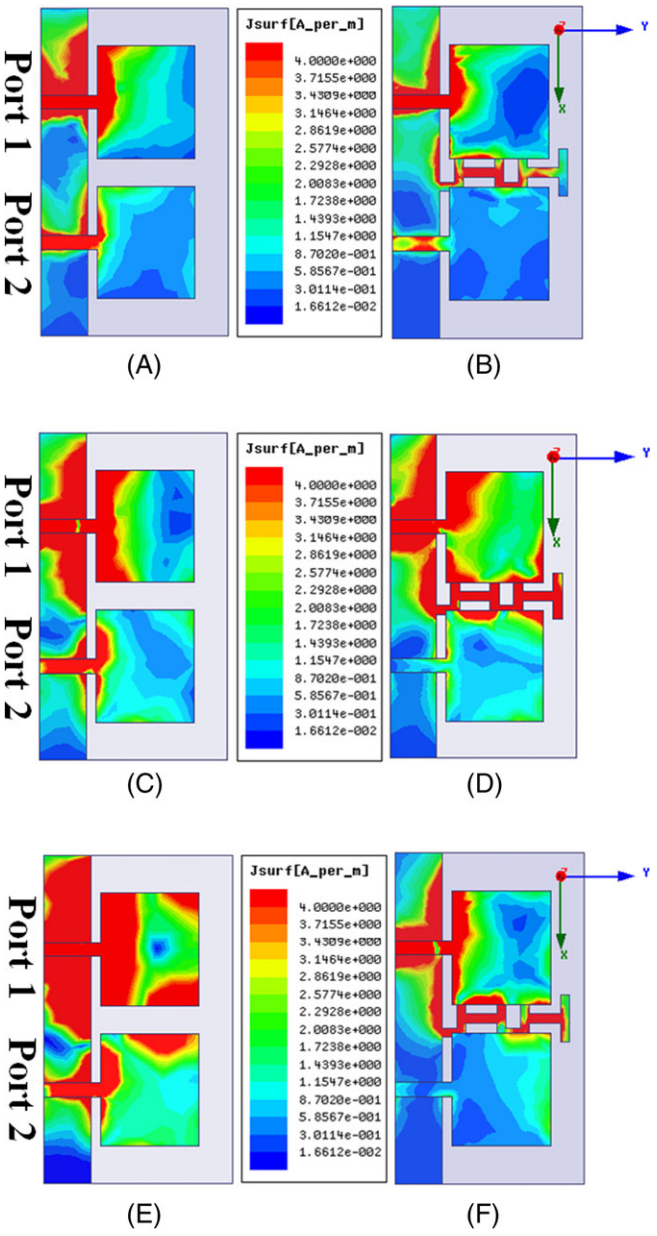

FIGURE 9 Surface current distributions of MIMO antenna 2.4 GHz (A) without stub (B) with stub, at 6 GHz (C) without stub (D) with stub and at 6.425 GHz (E) without stub (F) with stub on the ground plane

3.2 | Characterization as MIMO

Although the MIMO antenna provides reflection, isolation, radiation properties, it primarily works for multiplexing and

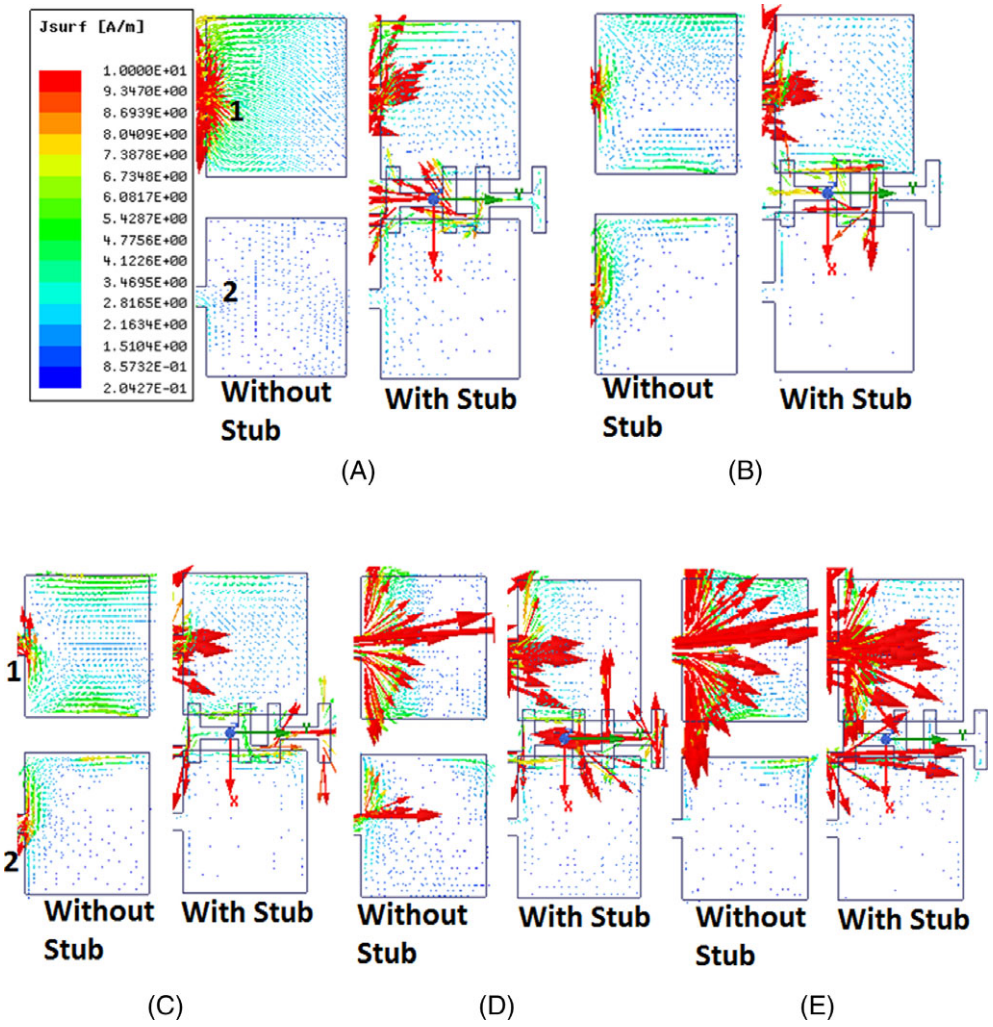

FIGURE 10 Characteristic-current of MIMO antennas (A) J1, (B) J2, (C) J3, (D) J4, and (E) J5 modes

diversity applications.[21] The envelope correlation coefficient (ECC) is the fundamental aspect that estimates the diversity performances in MIMO antenna systems.[22] To confirm the competency of the design as MIMO antenna application, it should attain very low ECC. The measurement of ECC describes the amount of isolation and correlation between the line communications.[23] The calculation of this ECC is obtained by using the subsequent Equation 1[24]:

$$\mathrm{ECC} = \frac{\left|S_{11}^{*}S_{12} + S_{21}^{*}S_{22}\right|^{2}}{\left(1-|S_{11}|^{2}-|S_{21}|^{2}\right)\left(1-|S_{22}|^{2}-|S_{12}|^{2}\right)} \quad (1)$$

For practically uncorrelated MIMO antenna, the acceptable diversity gain limits the ECC below 0.5.[25] Figure 7A shows the ECC features of the proposed antenna obtained from the measured S-parameters. It is observed from the figure that the ECC value is less than 0.01 throughout the complete operating band. Thus, the MIMO antenna confirms a good multiplexing performance to ensure the boosted data rate.

The diversity gain (DG) of the MIMO antenna is also a very crucial parameter to analyze the MIMO antenna performances. We can calculate the diversity gain by applying the following relation as given in Equation 2.[26]

$$\mathrm{DG} = 10\sqrt{1-(\mathrm{ECC})^{2}} \quad (2)$$

According to equation, the envelope correlation is used to compute the diversity performance of the designed MIMO antenna. Figure 7A illustrates the diversity gain with the variation of the frequency. It is noticed that the proposed MIMO antenna has very higher diversity gain (DG > 9.6).

Another important parameter is total active reflection coefficient (TARC) to analyze the characteristics of MIMO antenna. It is more significant quantity as compared to simple reflection coefficient.[27] TARC is composed of all the information related to the scattering parameters for a multiport radiating system.[28] The effective impedance bandwidth, resonating behavior and input excitation vector of the MIMO antenna can be realized by the TARC. It may

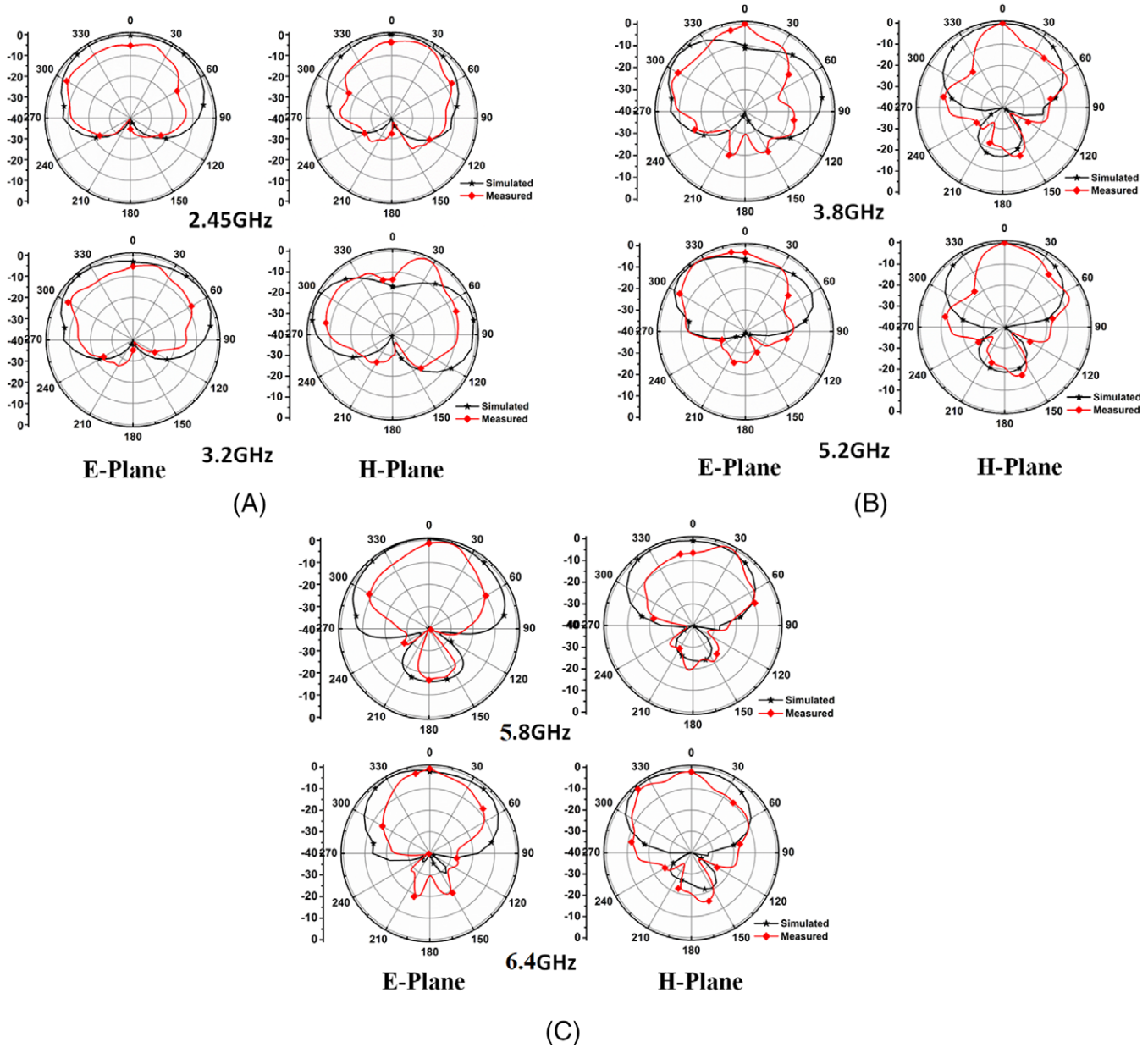

FIGURE 11 Normalized radiation patterns of the proposed antenna at (A) 2.45 and 3.2 GHz, (B) 3.8 and 5.2 GHz, and (C) 5.8 and 6.4GHz

be evaluated for a two-port MIMO antenna from the Equation 3,[28,29]

$$\mathrm{TARC} = \frac{\sqrt{\left(|(S_{11} + S_{12}e^{j\theta})|^2 + |(S_{21} + S_{22}e^{j\theta})|^2\right)}}{\sqrt{2}} \quad (3)$$

where θ denotes the phase angle of the excitation at the excitation port, S_{11} is the input reflection coefficient and S_{12} and S_{21} represent the port isolation. We investigate the resonance characteristics of the proposed MIMO antenna by picking up some of the arbitrarily chosen excitation phase angles. Figure 7B illustrates the TARC curve of the designed MIMO antenna. The proposed wearable MIMO antenna is normally attached with the human body or any other animals, which may be in moving condition. Therefore, phase angle of the input signal may be different at different positions. Here nine different excitation phase angles such as 5°, 20°, 30°, 55°, 70°, 90°, 120°, 150°, and 180° are considered. From Figure 7B, it is observed that the TARC curve provides stable resonance characteristic and impedance bandwidth for the entire set of phase angles. It confirms no significant degradation in antenna performances while moving with the body attached arrangements.

The channel capacity loss (CCL) and mean effective gain (MEG) are also very relevant for the characterization of the

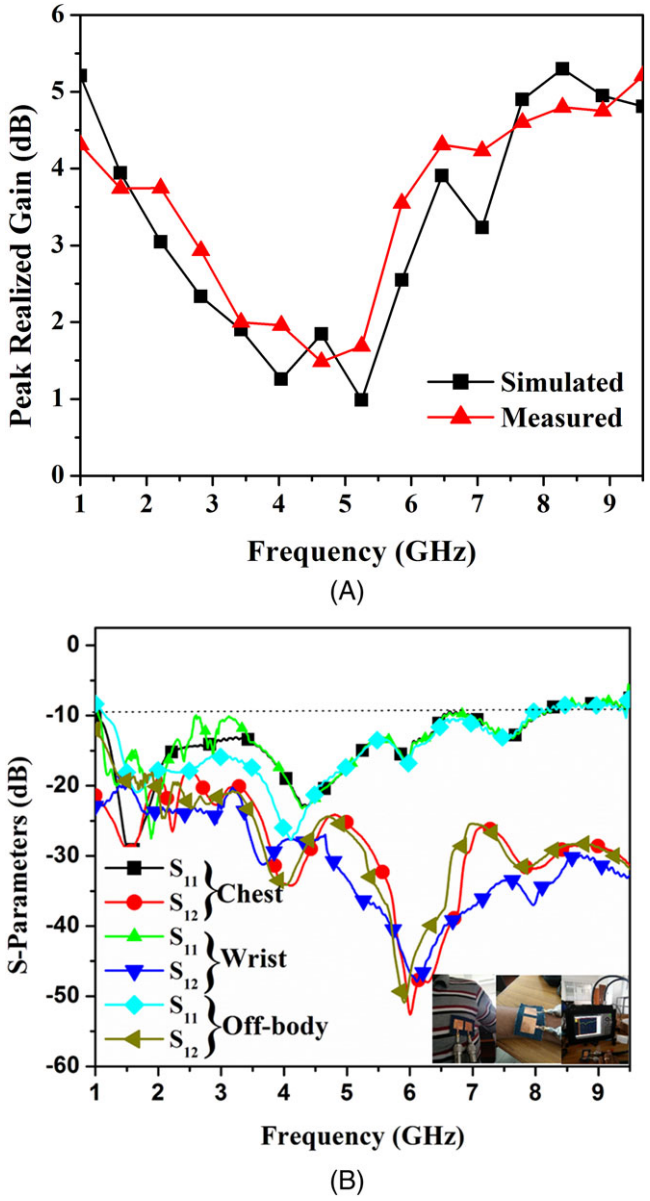

FIGURE 12 (A) Variation of simulated and measured gain of the suggested antenna with frequency and (B) measured S-parameters of the suggested antenna on chest, wrist, and off-body

MIMO antenna. Normally the data rate is higher in MIMO antenna as compared to a single element antenna. Therefore, investigation of CCL is important in the designed textile MIMO antenna. CCL is liable for the concentrated information level. This indicates that the transmission of information is promising uninterruptedly over the communication system. The CCL value of 0.4 or less is acceptable. The investigation of mean effective gain (MEG) describes the diversity characteristics of a wireless environment of the MIMO antenna. It supports clarification associated to the gain of the antenna. For good MIMO performances the MEG ratio (MEG1/MEG2) of port 1 and 2 of the proposed antenna should be ±3 dB. The CCL and MEG are evaluated according to the procedure as mentioned in Reference 4. Both the CCL and MEG are plotted and shown in Figure 8. From the figure, it is found that the value of CCL is less than 0.19 BPS/Hz and MEG ratio (MEG1-MEG2) is within ±2.53 dB. These ensure the good diversity performance of the designed wearable MIMO antenna.

3.3 | Surface current distribution

For the proposed textile constructed MIMO antenna system, the surface current distributions are investigated at three different frequencies 2.4 GHz, 6 GHz, and 6.425 GHz within the application band. We have done the analysis for the benefit of understanding the mutual coupling reduction between the ports. This also helps to determine the location of the used stub on the ground surface. The surface current distributions with and without 'I' shaped stubs are depicted in Figure 9A-F. It is effortlessly observed from Figure 8 that the 'I' shaped stub can reduce the coupling current between the elements and provide very high port isolation.

3.4 | Modal characteristics

The modal investigation of antenna clarifies the current distribution and radiation properties at different modes. The Eigen mode solver produces the surface current of the different modes of antenna. It determines the resonant frequencies and field patterns. The characteristic modes in other words are characteristic currents, which may be found as the Eigen functions of the weighted Eigen-value as given in Equation 4.[30]

$$X\left(\vec{J}_n\right) = \lambda_n R\left(\vec{J}_n\right) \tag{4}$$

Here λ_n is the nth eigenvalue, the J_n is the nth Eigen-currents, R is the real and X is the imaginary parts of the impedance operator $Z = R + JX$. The important effects that should be taken into account in Equation 4, is the way by which the eigenvalues react to modify the resonant frequency. Smallest magnitudes of λ_n are more important in the context of radiation problems and scattering problems.

TABLE 2 Some features of the proposed MIMO antenna

Op. Freq. (GHz)	S_{11} minima (dB)	S_{12} (dB)	Gain (dB)
2.4	−18.1	−22	3.75
3.2	−16.2	−20.9	2.42
3.7	−19.7	−30.1	1.93
5.15	−16.2	−27.8	1.68
5.72	−14.2	−41.4	2.71
5.925	−16.6	−53	3.54

TABLE 3 Assessment with some of the similar recent works

Design	Board (mm^2)	Op.Frqn. (GHz)	BW (GHz)	Max gain	Port Iso.(dB)
[5]	$\pi \times (21.1)^2$	2.4-2.49	0.09	4.2 dBi	>15
[14]	30 × 30	2.37-2.52	0.15	NA	>20
[15]	38.1 × 38.1	2.3-2.8	0.50	2.79 dBi	12
[16]	92.3 × 101.6	2.367-2.53, 5.147-5.863	0.163 0.716	5.8 dB	LB 20 UB 35
[17]	40 × 40	3.3-3.6, 4.5-5.0	0.3, 0.5	NA	>17
Prop.	40 × 70	2.4-8.0	5.16	4.4 dB	Min. 22 Max. 53

Figure 10A-E represents the modal current of the MIMO antenna with and without 'I' shaped stub. First five modes of both the antennas are analyzed. In mode J5, the current distribution near the feed is found to be higher as compared to the J1, J2, J3, and J4. It has less radiating behavior as compared to the other modes. Therefore, this resonant frequency has no reflection for the antenna design. The first and second mode J1 and J2 have vertical currents. They have directional radiating nature. The J3 and J4 modes resonate at higher frequencies. It is observed from the modal current analysis that the coupling current is less distributed whereas the 'I' shaped stub is used in the MIMO antenna.

3.5 | Radiation characteristics

In this section, the radiation characteristics of the proposed MIMO antenna for E and H-plane are investigated. The normalized measured and simulated two dimensional radiation patterns at 2.45 GHz, 3.2 GHz, 3.8 GHz, 5.2 GHz, 5.8 GHz, and 6.4 GHz are plotted in Figure 11A-C. Measured and simulated pattern characteristics are almost similar. It is notable that the patterns with the basic antenna structure are directed. It is realized from Figure 11A, that the antenna shows directional radiation characteristics at 2.45 GHz and 3.2 GHz whereas at 3.8 GHz, 5.2 GHz, and 6.4 GHz, the back-side radiations are found to be very small. The simulated and measured gain variations with frequency are depicted in Figure 12A. The maximum realized gain of the MIMO antenna is found to be around 4.4 dB at 6.4 GHz. In WLAN 2.4 GHz band, the maximum gain of 3.75 dB is obtained at 2.4 GHz whereas the maximum gain of 3.2 dB is obtained at 5.825 GHz in WLAN 5 GHz band. The deviation of the measured gain is due to in-house manual manufacturing error and the consumption of adhesive material to attach the copper element with the Jeans substrate. Furthermore, for the manual positioning of the copper element on the both side of the substrate, error may introduce by the cable loss in the system. The characteristics of the suggested MIMO antenna are abridged in Table 2.

3.6 | On-body effects on the proposed MIMO

The proposed textile MIMO antenna is placed on different position of the human body and scattering parameters are measured using Anritsu Vector Network Analyzer with model no. MS2037C/15/509. These outcomes are shown in Figure 12B. Wearable antennas must confirm to the high immunity of the human-body loading. Therefore, we have tried to investigate the on-body antenna characteristics by placing the prototype on two different positions of human body (such as chest and wrist). In Figure 12B, the measured on-body effects are compared with the of-body outcomes, where the antenna response does not exhibit significant deviations in the desired frequency bands. This may be due to the almost flat surface of the chest and wrist with compared to the antenna dimensions. However, the characteristics will differ from the lower value of the bending radius.

A comparison with a number of related recent researchworks is summarized in Table 3. The designed wearable MIMO antenna can be used as RF energy harvester by employing a matching or filter network and a rectifier circuitry within it. As it is wearable in nature therefore, it may be used in most of the suffering surroundings. Energy harvesting will be more effective in this confrontational situation. Therefore, future scope of this work may include the design of the additional circuitry of matching network and rectifier to operate the antenna as a rectenna for energy harvesting decorum. The antenna can also work for the low power IoT devices by placing it in a remote location to operate in the WLAN and WiMAX bands.

The work is mainly intended to design a low cost simple body wearable MIMO antenna with very small interelement spacing. In comparison to the other works, the present work provides very good −10 dB bandwidth in

the range of 1.83 to 8 GHz that covers the WLAN, WiMAX, C-band downlink and uplink bands.

4 | CONCLUSION

In this article, a double element wide band textile MIMO antenna with very low mutual coupling is investigated using two 'I' shaped ground stubs. The novelty of the design is; the textile strategy provides very high port isolation of greater than 22 dB throughout the entire operating band with the element spacing of 0.048λ. The proposed antenna provides very low envelope correlation coefficient (ECC < 0.01) and higher diversity gain (DG > 9.6). The design may be used for the WLAN (2.4 to 2.484 GHz/5.15 to 5.35 GHz /5.725 to 5.825 GHz), WiMAX (3.2 to 3.85 GHz), C-band downlink, and uplink (3.7 to 4.2 GHz/5.9 to 6.425 GHz) communication. Moreover, the antenna system provides a large fractional bandwidth of about 125.5% with on-body or off-body conditions. The wearable textile antenna structure is very simple. The advantage of this antenna is in-house manual fabrication is possible. From the results and discussions, it is clear that the design is suitable to use for the on-body and off-body WLAN, WiMax, C-band downlink, and uplink applications.

ORCID

Ashim Kumar Biswas https://orcid.org/0000-0002-5201-2420

REFERENCES

1. Yan S, Vandenbosch GAE. Radiation pattern-reconfigurable wearable antenna based on metamaterial structure. *IEEE Antennas Wirel Propag Lett*. 2016;15:1715-1718.
2. Panda AK, Sahu S, Mishra RK. A compact dual band 2 × 1 metamaterial inspired MIMO antenna system with high port isolation for LTE and WiMAX applications. *Int J RF Microw Comp Aid Eng*. 2017;27(8):e21122.
3. Luo CM, Hong JS, Zhong LL. Isolation enhancement of a very compact UWB MIMO slot antenna with two defected ground structure. *IEEE Antennas Wirel Propag Lett*. 2015;14:1766-1769.
4. Biswas AK, Chakraborty U. Reduced mutual coupling of compact MIMO antenna designed for WLAN and WiMAX applications. *Int J RF Microw Comp Aid Eng*. 2018;29:e21629. https://doi.org/10.1002/mmce.21629.
5. Wen D, Hao Y, Munoz MO, Wang H, Zhou H. A compact and low-profile MIMO antenna using a miniature circular high-impedance surface for wearable applications. *IEEE Trans Antennas Propag*. 2018;66(1):96-104.
6. Gao GP, Hu B, Tian XL, Zhao QL, Zhang BT. Experimental study of a wearable aperture-coupled patch antenna for wireless body area network. *Microw Opt Tech Lett*. 2017;59(4):761-766.
7. Ali WA, Mansour AM, Mohamed DA. Compact UWB wearable planar antenna mounted on different phantoms and human body. *Microw Opt Tech Lett*. 2016;58(10):2531-2536.
8. Salam A, Khan AA, Hussain MS. Dual band microstrip antenna for wearable applications. *Microw Opt Tech Lett*. 2014;56(4):2531-2536.
9. Xiaomu H, Yan S, Vandenbosch GAE. Wearable button antenna for dual-band WLAN applications with combined on and off-body radiation patterns. *IEEE Trans Antennas Propag*. 2017;65(3):1384-1387.
10. Malathi ACJ, Thiripurasundari D. Review on isolation techniques in MIMO antenna systems, Indian. *J Sci Tech*. 2016;9(35):1-10.
11. Grau L, Andujar A, Anguera J. On the isolation of a MIMO 2 × 2 antenna system using non-resonant elements: 1.71 GHz–2.69 GHz case study. *Microw Opt Tech Lett*. 2017;59(6):2348-2353.
12. Bardera EC, Fernandez MS, Talegon LA, Delgado AV. (2016). Feasibility of a wearable textile antenna hub based on massive MIMO systems. In Proc. of the 18th Mediterranean Electrotech. Conf, MELECON 2016; Limassol, Cyprus; 2016:1-6.
13. Abdalla MA, Ibrahim AA. Design and performance evaluation of metamaterial inspired MIMO antennas for wireless applications. *Wirel Pers Commun*. 2017;95:1001-1017.
14. Alkhamis R, Wigle J, Song H. Global positioning system and distress signal frequency wrist wearable dual-band antenna. *Microw Opt Tech Lett*. 2017;59(8):2055-2064.
15. Qu L, Piao H, Qu Y, Kim HH, Kim H. Circularly polarised MIMO ground radiation antennas for wearable devices. *Electron Lett*. 2018;54(4):189-190.
16. Li H, Sun S, Wang B, Wu F. Design of compact single-layer textile MIMO antenna for wearable applications. *IEEE Trans Antennas Propag*. 2018;66(6):3136-3141.
17. Yan S, Soh PJ, Vandenbosch GAE. Dual-band textile MIMO antenna based on substrate-integrated waveguide (SIW) technology. *IEEE Trans Antennas Propag*. 2015;63(11):4640-4647.
18. Zhu L, Hwang HS, Ren E, Yang G. High performance MIMO antenna for 5G wearable devices. IEEE International Symposium on Antennas and Propagation & USNC/URSI National Radio Science Meeting; San Diego, CA; 2017:1869-1870.
19. *HFSS ver.17*. Pittsburgh, PA: Ansoft Corporation.
20. Sankaralingam S, Gupta B. Determination of dielectric constant of fabric materials and their use as substrates for design and development of antennas for wearable applications. *IEEE Trans Instrum Meas*. 2010;59(12):3122-3130.
21. Li Y, Sim CYD, Yang G. 12-Port 5G massive MIMO antenna array in sub-6GHz mobile handset for LTE bands 42/43/46 applications. *IEEE Access*. 2017;6:344-354.
22. Zhu J, Li S, Feng B, Deng L, Yin S. Compact dual-polarized UWB quasi-self-complementary MIMO/diversity antenna with band-rejection capability. *IEEE Antennas Wirel Propag Lett*. 2016;15:905-908.
23. Luo CM, Hong JS, Zhong LL. Isolation enhancement of a very compact UWB-MIMO slot antenna with two defected ground structures. *IEEE Antennas Wirel Propag Lett*. 2015;14:1766-1769.
24. Chacko BP, Augustin G, Denidni TA. Uniplanar slot antenna for ultrawideband polarization-diversity applications. *IEEE Antennas Wirel Propag Lett*. 2013;12:88-91.
25. Han M, Choi J. Small-size printed MIMO antenna for next generation mobile handset application. *Microw Opt Technol Lett*. 2011;53(2):248-352.

26. Iqbal A, Saraereh OA, Ahmad AW, Bashir S. Mutual coupling reduction using F-shaped stubs. *IEEE Access*. 2017;6:2755-2759.
27. Aouadi B, Tahar JB. Requirements analysis of dual band MIMO antenna. *Wirel Pers Commun*. 2015;82:35-45.
28. Das G, Sharma A, Gangwar RK. Dual port aperture coupled MIMO cylindrical dielectric resonator antenna with high isolation for WiMAX application. *Int J RF Microw Comp Aid Eng*. 2017;27 (7):e21107.
29. Su S, Lee C, Chang F. Printed MIMO-antenna system using neutralization-line technique for wireless USB-dongle applications. *IEEE Trans Antennas Propag*. 2012;60(2):456-463.
30. Harrington RF, Moutz JR. Theory of characteristic mode for conducting bodies. *IEEE Trans Antennas Propag*. 1971;19(5): 622-628.

AUTHOR BIOGRAPHIES

Ashim Kumar Biswas received BTech from Kalyani Govt. Engineering College and MTech from the University of Burdwan, India, respectively, all in Electronics and Communication Engineering (ECE) Department. He has several years of teaching experience. Presently he is working towards the PhD degree in National Institute of Technology, Silchar, Assam. He has published a few numbers of research papers in reputed journals and conference proceedings. His research interests include microstrip antenna, DGS, EBG, MIMO, wearable antennas, and so forth.

Ujjal Chakraborty received BTech and MTech from the University of Burdwan and PhD from National Institute of Technology, Durgapur, India in the Department of Electronics and Communication Engineering. He is presently associated with the Department of Electronics and Communication Engineering in National Institute of Technology, Silchar, Assam, India and holds the post of Assistant Professor. He has more than 14 years of teaching experience. He has authored and co-authored more than 50 peer-reviewed scientific papers published in national and international journals and conferences. His research interest includes the metamaterial antennas, phased array antennas, body wearable conformal antennas, and MIMO antennas.

How to cite this article: Biswas AK, Chakraborty U. A compact wide band textile MIMO antenna with very low mutual coupling for wearable applications. *Int J RF Microw Comput Aided Eng*. 2019;e21769. https://doi.org/10.1002/mmce.21769